
Image Sensor-Driven Circuit Design for Measuring Optical Frequency Comb Spectrum

*Yingqiu HE **

College of Science
Zhejiang University of Technology
Hangzhou, China

Kaoru MINOSHIMA

Department of Engineering Science
The University of Electro-Communications
Tokyo, Japan

Abstract

The study focuses on developing an image sensor-driven circuit for measuring the spectral information of optical frequency comb which is one of ultrashort laser sources. The paper presents the sensor circuit design details and the spectrum measuring method. Experimental results included the analysis of the video signal for evaluating the sensor under different operating conditions. Finally we discuss the points for improvement of driven circuit design and further research after measuring the spectrum.

Keywords: Image sensor, Circuit design, Optical frequency comb spectrum

1 Introduction

The optical spectrum of a light source contains information on how the optical energy or power is distributed over different wavelengths or frequencies. A pulse train generated by a mode-locked laser has a spectrum consisting of a large number of well-defined, equally spaced series of sharp lines, known as an optical frequency comb (OFC) which has been widely applied in many fields, like astronomy [1], medical diagnostics [2], precise distance measurement [3] and so on. Figure 1 shows the OFC pulses both in the time domain and frequency domain, with the optical frequencies (f_n) are defined in

$$f_n = nf_{\text{rep}} + f_{\text{ceo}},$$

where f_{rep} is the repetition frequency producing pulses and f_{ceo} is the comb carrier-envelope offset frequency due to the pulse-to-pulse phase shift. With the rapid rise of OFC, many applications have also developed rapidly, including three-dimensional (3D) imaging technology [4] applied from agriculture and medicine to entertainment and security. After K. Minoshima [5] successfully demonstrated the feasibility of 3D

imaging using chirped pulse lasers, our group [6-8] presented a novel one-shot imaging technique which utilizes an OFC-based light source to achieve high image resolution, fast acquisition speed, and wide dynamic range. The technique detects the spectral interference fringe to obtain the phase difference for further research goal. For real-time and high-resolution image processing, two precisely phase-shifted interference fringes need to be detected to extract amplitude and phase information of the fringe. Therefore, two image sensors are needed to detect the set of spectral interference fringes simultaneously to obtain the precise phase difference to enhance the image quality. A precise optical signal detection system is therefore required.

This study aims at developing an image sensor driven circuit to detect the light and installing the circuit to a spectrometer for measuring the near-infrared spectral information of the OFC pulse beam. The InGaAs linear image sensor [9], or line sensor, used in the study is specifically designed for near-infrared detection realizes both high-speed readout and high gain. Comparing to previous circuit, this circuit could detect light with lower noise and higher accuracy. The paper presents the sensor circuit de-

*The author is supported by JASSO Scholarship.

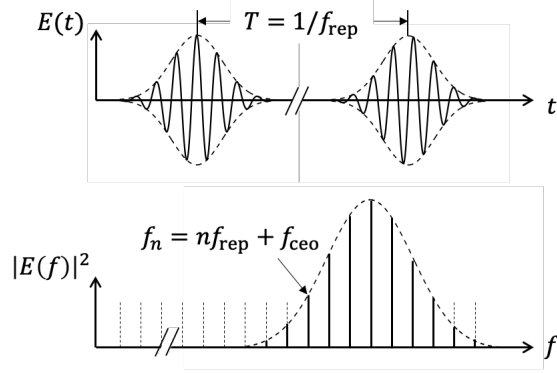


Figure 1: Diagram of the OFC presenting in the time and frequency domains.

sign and the materials used in the experiments, along with an analysis of the characteristics of the video signal obtained with light from an infrared LED incident on the image sensor. This analysis also includes the impedance matching problem typically encountered in relatively high frequency circuits, as well as the performance of the video signals in relation to the integration time and conversion efficiency of the sensor. After evaluating the circuit, the spectrum of the OFC is expected to be obtained by installing the circuit to a spectrometer. Future work includes refining the circuit design and applying it to the 3D imaging experimental setup to improve performance and enable enhanced imaging capabilities within the research group.

2 Method

2.1 Driven Circuit

The InGaAs linear image sensor G11508-512SA series (hereafter referred to “sensor”) used in the experiments operates by generating electric charges in its photodiodes (PDs) when light enters. These charges flow into a charge amplifier and output signals. The PDs detect incident light, capturing power information for each individual pixel. The sensor consists of 2 lines, with each line containing 256 pixels. To drive the sensor, digital inputs in the form of a master clock pulse (CLK) and integration time control pulse (Reset) are required. Because two control signals must be H-COMS level inputs, one level shifter (LS) is added to change 3.3 Volts to 5.0

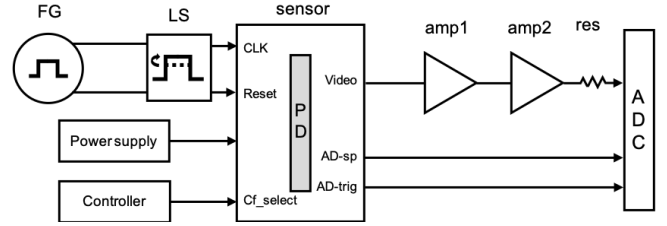


Figure 2: Diagram of the circuit. (amp1: buffer op-amplifier; amp2: differential op-amplifier; res: resistor)

Volts after the function generator (FG) generating 3.3Volts. The sensor outputs an analog video signal (Video) as well as digital outputs (AD_trig, AD_sp) for sample-and-hold purposes. A buffer amplifier for enhancing sensor drive capability and a differential amplifier for compensating sensor offset voltage are needed before being fed to an oscilloscope or an analog-to-digital converter (ADC). Figure 2 displays the diagram of the circuit. Additionally, Figure 8 presents the schematic of the driving circuit, including the materials used.

To assess the characteristics of the sensor and evaluate the circuit under different operating conditions, the experiments follows several checking steps: (1) Output signals: The Video, AD_trig and AD_sp signals are output by employing integration then readout method. (2) Integration time: It is determined by the pulse width of the Reset signal and have an effect with Video intensity. (3) Conversion efficiency: The sensor offers two gain options: “ $\times 1$ ” and “ $\times 10$ ”. The desired gain can be selected by controlling the Cf_select pin using external voltage. (4) Impedance Matching: The issue is a common consideration in radio frequency circuit. The output signals exhibit high impedance, necessitating the use of a buffer amplifier. Additionally, a resistor is added after the amplifiers to ensure impedance matching.

2.2 Spectrometer

The Figure 3 illustrates the diagram of a spectrometer designed by a previous student T. Morito, which is used to measure the spectrum of the OFC light source. In the setup, two light beams are guided through two single mode fibers (SMFs)

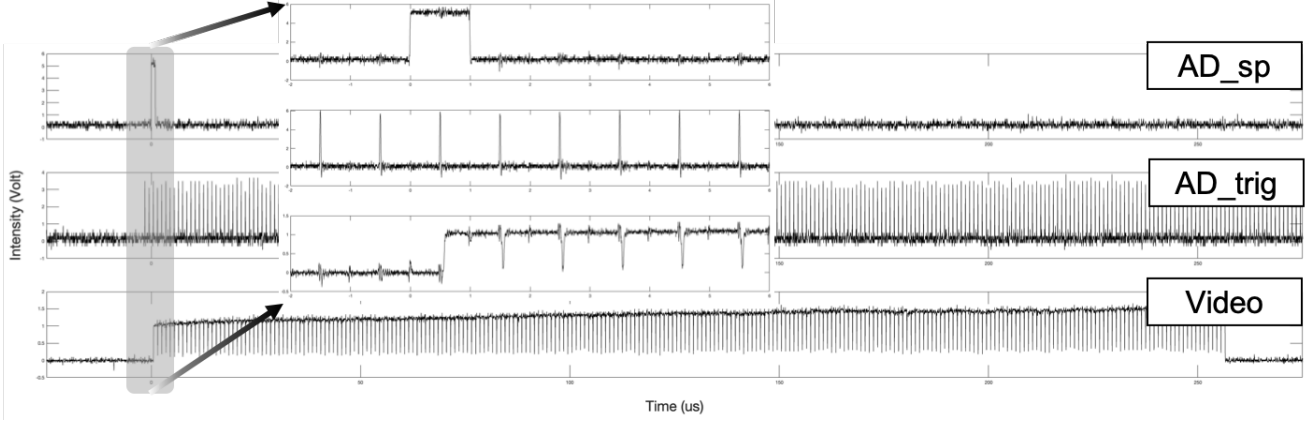


Figure 3: Overview of the output signals of AD_sp, AD_trig and Video detected from an infrared LED and expansion of the parts of few pixels.

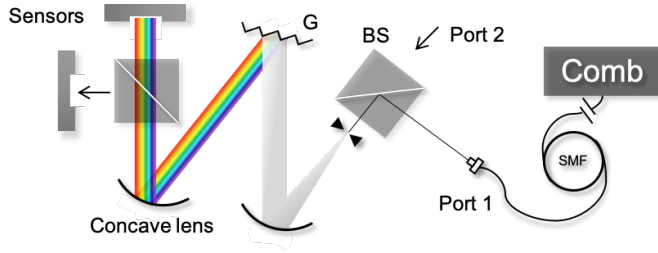


Figure 4: Diagram of the spectrometer.

from two ports and detected by two sensors. The height difference between the beams from optical table prevents their interaction. After ejecting from the fiber, a quarter-wave plate and a half-wave plate are expected to use here in the future for adjust the beam polarization to maximize grating efficiency. The beams then pass through a beam splitter (BS) and are shaped by a slit. Using two concave lens, each with a focal length of 100 mm, the beam is focuses before and after the diffraction grating (G) used for separating polychromatic light into the underlying constituent wavelengths. Finally, the Video outputs from the sensors is analyzed to obtain the spectrum.

3 Results of Video Signal

Before installing the circuit to the spectrometer for measuring the comb spectrum, an infrared LED is used to check the circuit performance. The first step involves check the power supply line connected to the sensor. Following that,

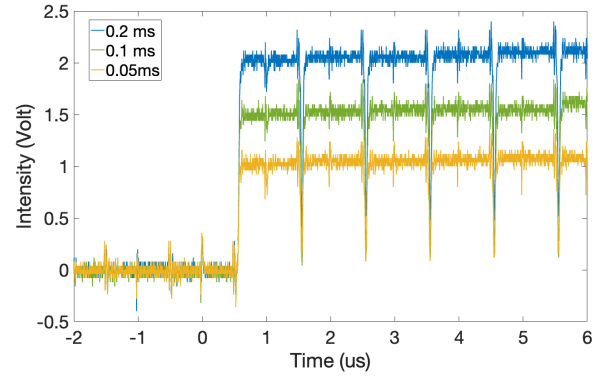


Figure 5: The Video detected with varying resolution time of 0.2, 0.1 and 0.05 ms within few pixels from 1 to 5.

the control signal of CLK and Reset are input from the function generator to drive the sensor. Throughout the entire experiment, the frequency of CLK input to sensor is maintained at 1 MHz. As a result, the Video readout frequency is also 1 MHz, indicating that each pixel is read out in 1 μ s of time. After driving the sensor, Figure 4 to 7 present the results of sensor evaluations.

1. Output signals: Figure 4 shows the output signals obtained during one complete readout period of 256 pixels. Additionally, it shows the signals form several pixels within the period, with an integration time of 0.1 ms. The maximum of intensity during test is approximately 2.8 Volts.

2. Integration time: By varying the frequency of Reset to 1 kHz and 2 kHz along with duty cycle of 10% and 20%, the integration time becomes equal to the width of Reset. The relative position of the sensor and light remains the same across the four groups. Figure 5 demonstrates that with a longer integration time, the intensity is increases, indicating that more light can enter each pixel and the sensor's sensitivity is higher. However, this also results in a lower speed of operation.
3. Conversion efficiency: When the Cf_select pin is connected to 5 Volts or GND, the conversion efficiency of the PDs changing from “ $\times 1$ ” to “ $\times 10$ ”. By using the formula of

$$\text{Gain} = 10 \log_{10}(\times 10 / \times 1),$$

it is possible to calculate the gain in each pixel. Figure 6 demonstrated that the factor of gain floating around 10 and proved the function of Cf_select pin.

4. Impedance matching: A resistor used here to match the impedance after the amplifiers. The Video is then measured both without and with the resistor, and their frequency spectra are compared using FFT algorithm in MATLAB. In Figure 7, the left side shows strong harmonic frequencies around 40 MHz, 70 MHz and 110 MHz, but after adding a resistor, the right side of the figure demonstrates that only a small intensity of high frequency signals remains, which indicates that the resistor helps mitigate the presence of unwanted harmonics.

4 Discussion

Comparing to previous driven circuit, the current circuit improve the quility of signls detected with lower noises and higher accuracy. However, the current results reveal that the residual unwanted signals in the Video output are still existed. To solve this issue, several improvements are proposed, including using a power supply line with higher sufficiency ability to drive current or inserting an RC low pass filter after the

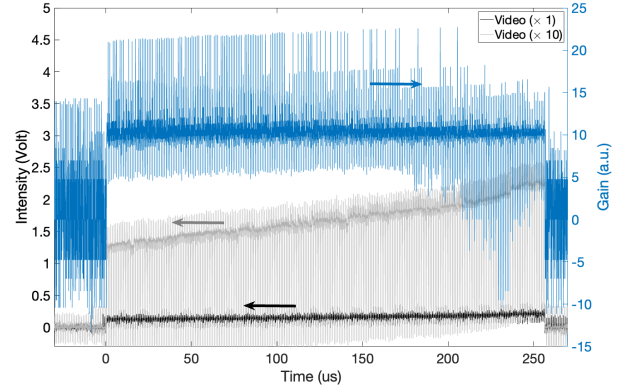


Figure 6: The Video detected with conversion efficiency of $\times 1$ and $\times 10$ and the calculated gain around 10.

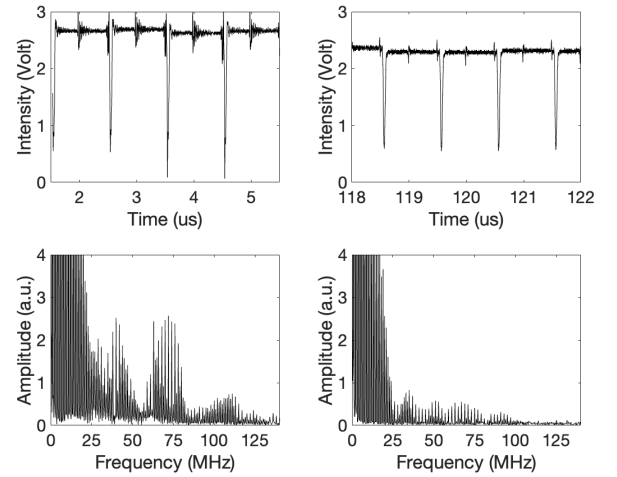


Figure 7: The Video detected without (left) and with (right) the resistor with 256 pixels and their FFT spectrum in the bottom.

amplifier output to reduce noise. Future work for the circuit includes using an FPGA (Field-Programmable Gate Array) for pulse generation instead of a function generator and to analyze the Video output instead of relying on an oscilloscope.

The aim of this study is to measure the spectrum of the OFC in a spectrometer setup rather than using Optical Spectrum Analyzer, because it was motivated by the final goal of the setup, which is measuring the spectral interference pattern of two OFC pulses beams and analyze the phase difference between them. The phase difference information is then used to give feedback

to the OFC to adjust the frequencies for achieving a higher quality of 3D imaging. Therefore, all the mentioned improvements and approaches were aimed at the ultimate goal of our group research. More detailed information on the techniques and methods employed can be found in reference [8].

5 Conclusions

In conclusion, this study developed an image sensor driven circuit for detecting incident light, which is expected to apply it into a spectrometer for measuring the OFC spectrum for further research goal. Four testing results including integration time and conversion efficiency provided insights into driving the sensor under various conditions of different infrared light source. The study also addressed the important aspect of impedance matching in the RF circuit design by adding a reasonable resistor. Future work includes install the driven circuit into the member-made spectrometer for analyzing the phase difference of two OFC pulse beams and approach the goal of higher resolution of 3D imaging. Overall, it is hoped that this study can contribute positively to the research group's goals and objectives.

6 Acknowledgments

The author expresses gratitude to JASSO scholarship, Prof. Kaoru Minoshima for research opportunity and academic guidance, and Assoc. Prof. Takashi Kato, Yasushi Nekoshima, Keito Hino, Dr. Haochen Tian for experimental assistance. Special thanks to all members of Minoshima lab, JUSST program, UEC Aikido club and my family for supporting and encouragement during this one year.

References

[1] M. Andrew, A. Tyler, F. B. Chad, B. Scott, B. Wesley, "Stellar spectroscopy in the near-infrared with a laser frequency comb", *Optica* 6, 233-239, 2019.

[2] J.T. Michael et al, "Cavity-enhanced optical frequency comb spectroscopy: application to human breath analysis", *Optics Express* 16, 2387-2397, 2008.

[3] E.D. Caldwell, L.C. Sinclair, N.R. Newbury et al, "The time-programmable frequency comb and its use in quantum-limited ranging", *Nature* 610, 667-673, 2022.

[4] E. Vicentini, Z. Wang, K. Van Gasse et al, "Dual-comb hyperspectral digital holography", *Nat. Photon.* 15, 890-894, Nov. 2021.

[5] K. Minoshima et al, "Simultaneous 3-D Imaging Using Chirped Ultrashort Optical Pulses", *Jpn. J. Appl. Phys.* 33 L1348, 1994.

[6] T. Kato, M. Uchida, Y. Tanaka, K. Minoshima, "Non-scanning three-dimensional imaging using two-dimensional spectroscopy and spectral interferometry with a chirped frequency comb", *CLEO-PR*, Singapore, 2017, pp. 1-2.

[7] T. Kato, M. Uchida, Y. Tanaka, K. Minoshima, "High-resolution 3D imaging method using chirped optical frequency combs based on convolution analysis of the spectral interference fringe", *OSA Continuum* Vol. 3, No. 1, 15 Jan. 2020.

[8] T. Kato, H. Ishii, K. Terada, T. Morito, K. Minoshima, "Fully non-scanning three-dimensional imaging using an all-optical Hilbert transform enabled by an optical frequency comb", arXiv: 2006.07801 [physics.optics], Jun. 2020.

[9] <https://www.hamamatsu.com/us/en/product/optical-sensors/image-sensor/ingaas-image-sensor/ingaas-linear-image-sensor/G11508-512SA.html>

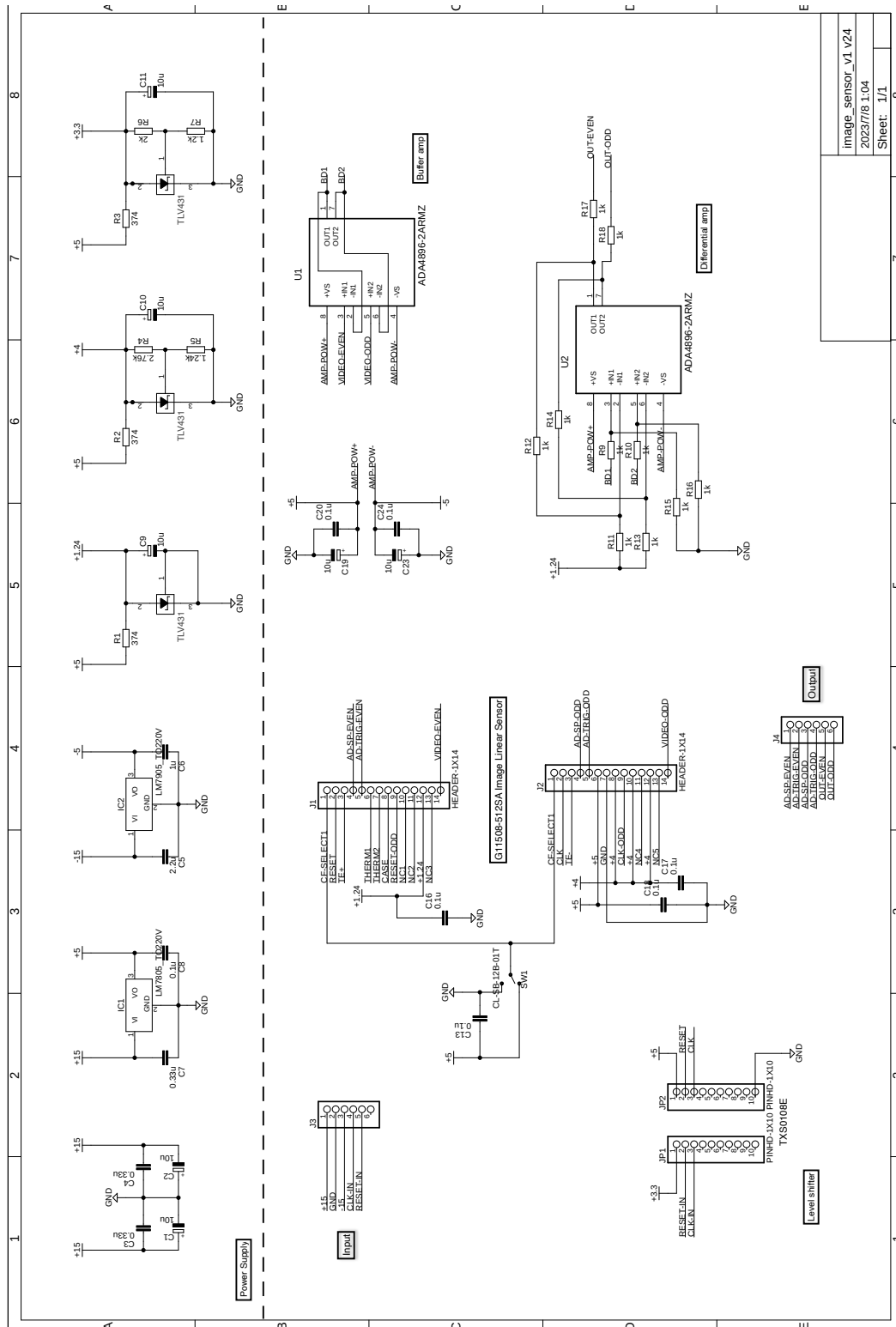


Figure 8: Schematic of the circuit.